

## Stability of screening solitons in photorefractive media

M. Facão\* and D. F. Parker†

*School of Mathematics and Statistics, University of Edinburgh, The King's Buildings, Edinburgh EH9 3JZ, United Kingdom*

(Received 28 February 2003; published 18 July 2003)

Normal mode stability of both rectilinear and self-bending photorefractive screening solitons is considered. In each case, the Evans function procedure is used to investigate stability and to search for internal modes. For the rectilinear case, a standard Evans function procedure is applied. However, in the self-bending case the asymptotic form of the eigenvalue problem is a system of Airy equations, instead of the usual system of constant coefficient differential equations. To overcome this difference, a modified version of the Evans function method, using Airy functions rather than exponentials, is implemented and applied. The results confirm stability and give an internal mode pattern in good agreement with full numerical integration.

DOI: 10.1103/PhysRevE.68.016610

PACS number(s): 42.65.Tg, 42.65.Sf, 42.70.Nq

### I. INTRODUCTION

Photorefractive solitons were predicted in 1992 [1] and were demonstrated one year later [2]. They are distinct amongst optical solitons in requiring only low power lasers, as small as  $\mu$ Ws, and elementary experimental apparatus. Photorefractive materials are doped electro-optic crystals that have electronic energy levels within the forbidden gap. The photorefractive effect consists of a reversible change of the refractive index induced by a spatial variation of an optical field, which is accomplished in two steps: creation of free charge by light absorption and charge migration by drift and diffusion. A photorefractive soliton is a beam that becomes self-trapped through the above mechanism, which may be interpreted as though the beam were inducing its own waveguide. Several mechanisms are possible, each one leading to a different kind of photorefractive soliton. Here we focus on the so-called *screening* photorefractive solitons. In this type, the photorefractive crystal is subjected to an external voltage orthogonal to the light propagation. The final charge distribution in the illuminated region produces a space-charge electric field  $E_{sc}$  with polarity opposite to the external field. The change in the refractive index that results from the electro-optic effect is given by  $\Delta n = n^3 r_{\text{eff}} E_{sc}$ , where  $n$  is the unperturbed refractive index and  $r_{\text{eff}}$  is an effective electro-optic coefficient. In turn, the space-charge field depends only on the beam power whenever only the drift produced by the external field is important, but depends also on the transverse spatial derivative of the beam power whenever the diffusion mechanism is appreciable. The first case produces symmetric beams propagating along rectilinear trajectories and occurs for high external voltage and narrow beams [3,4]. The latter produces slightly asymmetric beams propagating along a parabolic trajectory, usually known as *self-bending* solitons, and occurs for broader beams [5–7]. The only reported stability analysis of the *self-bending* solitons was based on simulations of the full evolution equation [5,6]. In this work we investigate their normal mode stability by a method similar to the standard Evans function method [8–10]. Unlike usual applications, the stability equations do not tend to con-

stant coefficient differential equations away from the beam, but instead they tend to a system of Airy equations. We have used the Airy functions to develop a modification to the Evans function method and have applied it in a search for stability eigenvalues of the self-bending solitons.

In Sec. II, we introduce the ordinary differential equation obtained from the partial differential equation by a similarity variable reduction and briefly describe the characteristic profiles for the two types of solutions: rectilinear and self-bending. The stability eigenvalue problem is presented in Sec. III, where we prove the stability of the rectilinear beams using the *Vakhitov-Kolokolov* criterion. Sections IV and V are devoted to the Evans function method. First, we find the internal modes of the diffusionless case applying the standard version of the method. Then we define a suitable Evans function for the diffusive case. Its application confirms the stability and gives the internal modes of the self-bending solutions. Finally, in Sec. VI, we present the results of numerical integration of the full evolution equation, which are in agreement with the normal mode stability analysis.

### II. MODEL AND LOCALIZED SOLUTIONS

Using the band transport model of the photorefractive effect by Kukhtarev and Vinetskii [11,12] to evaluate the space-charge field  $E_{sc}$  and considering the change of refractive index  $\Delta n = n^3 r_{\text{eff}} E_{sc}$ , we arrive at the following equation describing the evolution of the optical field [4,5]:

$$iq_z + q_{xx} - \frac{q}{1+|q|^2} + \gamma \frac{(|q|^2)_x q}{1+|q|^2} = 0, \quad (1)$$

where  $q$ ,  $z$ ,  $x$ , and  $\gamma$  are normalized versions of the complex beam envelope, propagation distance, transverse spatial coordinate, and diffusion parameter, respectively.

The above equation admits self-similar solutions having  $\eta = x - 2Vz + az^2$  as a similarity variable (with  $V$  and  $a$  constants) [7]. Thus, introducing the ansatz  $q(z, x) = \exp[i\theta(z, \eta)]F(\eta)$  into Eq. (1), with  $F$  and  $\theta$  real, and requiring that  $F \rightarrow 0$  as  $\eta \rightarrow \pm\infty$ , we obtain

$$F'' + \left[ B + a\eta - \frac{1}{1+F^2} + \gamma \frac{2FF'}{1+F^2} \right] F = 0 \quad (2)$$

and

\*Electronic address: M.M.Resende-Viera-Facao@sms.ed.ac.uk

†Electronic address: D.F.Parker@ed.ac.uk

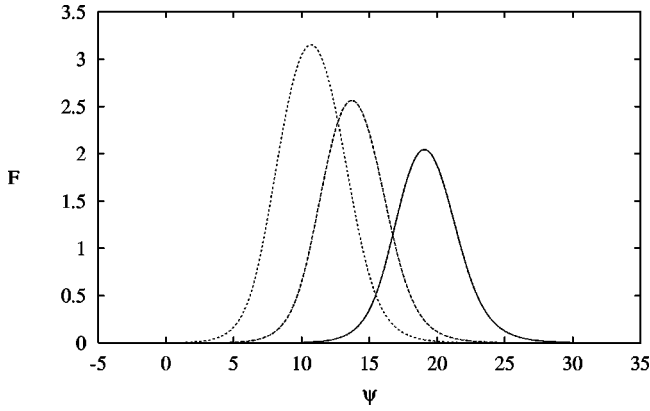


FIG. 1. Three beam profiles for  $\gamma=0.1$ , corresponding to points marked  $\circ$  in Fig. 2.

$$\theta(z, \eta) = (V - az)\eta + \frac{1}{3}a^2z^3 - aVz^2 + (V^2 - B)z + C, \quad (3)$$

where  $B$  and  $C$  are arbitrary parameters. For  $\gamma=0$ , the curvature parameter  $a$  should be equal to 0 and for each  $B$ , there then exists a family of solutions having peak amplitude  $\mu$  related to  $B$ , through  $B = \ln(1 + \mu^2)/\mu^2$ . They are symmetrical about the peak position  $\eta = \eta_0$  [3,4]. In the diffusive case,  $\gamma \neq 0$ , the curvature parameter is necessarily nonzero. The beam profiles result from the numerical integration of Eq. (2), using a shooting method [6,7]. The method uses estimates obtained from a perturbation procedure based upon the diffusionless profiles ( $\gamma=0$ ). The initial conditions for  $F$  and  $F'$  may be taken from the Airy functions in a way already used by Aleshkevich *et al.* [13] to treat the diffusive case of photorefractive solitons, but when the nonlinearity was of the Kerr type.

In the diffusive case, we transform Eq. (2) using  $a\psi = a\eta + B - 1$  so as to obtain an ordinary differential equation (ODE) without the parameter  $B$  as follows:

$$F'' + \left[ a\psi - \frac{F^2}{1+F^2} + \gamma \frac{2FF'}{1+F^2} \right] F = 0. \quad (4)$$

In fact, in the tail region where  $F \approx 0$ , Eq. (4) transforms to the Airy equation  $F'' - zF = 0$  by the change of variable  $z(\psi) = -a^{1/3}\psi$ . The only solutions that decay as  $z \rightarrow +\infty$  ( $\psi \rightarrow -\infty$ ) are multiples of  $\text{Ai}(z)$ . At the other extreme, both  $\text{Ai}(z)$  and  $\text{Bi}(z)$  decay algebraically and oscillatorily. Nevertheless, numerics on Eq. (4) give us beam profiles with rapid decay at either side. This suggests that the right tail of  $F$  is still in a region of positive  $z$  and is picking up the exponential behavior of  $\text{Bi}(z)$  for  $z > 0$ . The algebraically decaying oscillations should appear in the right tail only

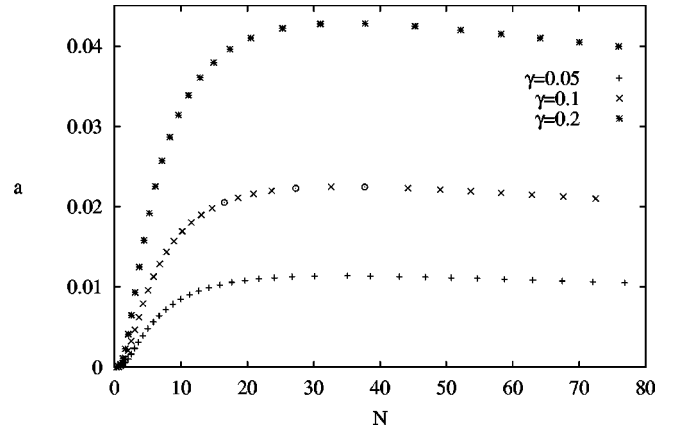


FIG. 2. Dependence of the curvature parameter  $a$  on the beam power  $N$ , for three values of  $\gamma$ .

when  $|F|$  is already very small. Hence, the initial conditions for numerical integration of Eq. (4) are chosen as

$$F(\psi_1) = c_1 \text{Ai}[z(\psi_1)] = \epsilon,$$

$$F'(\psi_1) = -c_1 a^{1/3} \text{Ai}'[z(\psi_1)],$$

where  $\psi_1$  is an estimate of the left tail position used in the shooting method. We were able, by adjusting  $\psi_1$ , to obtain localized solutions for  $\gamma$  up to 0.2 over a wide range of beam power  $N = \int_{-\infty}^{\infty} F^2 d\psi$ . Figure 1 shows three of these beam profiles with different peak amplitudes  $F_{\max}$ , for  $\gamma=0.1$ . For fixed  $\gamma$ , the solutions may be parametrized by the curvature parameter  $a$  or by the beam power  $N$ . The dependence of  $a$  on  $N$  is not monotonic but exhibits a maximum (see Fig. 2). For larger  $\gamma$ , beam profiles have also been computed, but for  $\gamma=0.3, 0.4$ , and  $0.5$  the numerical procedure fails to find profiles for increasingly wide intervals of  $N$ .

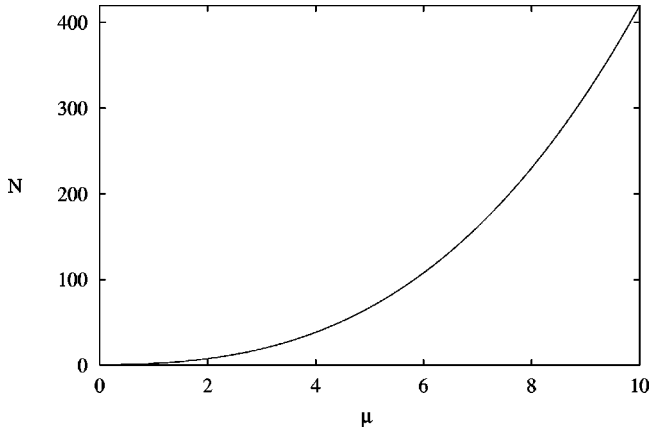
### III. NORMAL MODE STABILITY

In order to perform linear stability analysis, we consider a total solution of the form  $q(z, \eta) = \exp[i\theta(z, \eta)][F(\eta) + w(z, \eta)]$ , where  $F(\eta)$  is the real beam profile obtained from Eq. (2) and  $w(z, \eta)$  is a small complex perturbation term. Inserting the above form into Eq. (1), and seeking solutions in the form  $w(\eta, z) = u(\eta)e^{i\lambda z} + v^*(\eta)e^{-i\lambda^* z}$ , we obtain the following eigenvalue problem:

$$L \begin{pmatrix} u \\ v \end{pmatrix} = \lambda \begin{pmatrix} u \\ v \end{pmatrix}, \quad (5)$$

where the operator  $L$  is given by

$$L = \begin{pmatrix} \partial_{\eta\eta} + B + a\eta + \gamma \frac{F^2}{1+F^2} \partial_{\eta} + r(\eta) & \gamma \frac{F^2}{1+F^2} \partial_{\eta} + s(\eta) \\ -\gamma \frac{F^2}{1+F^2} \partial_{\eta} - s(\eta) & -\partial_{\eta\eta} - B - a\eta - \gamma \frac{F^2}{1+F^2} \partial_{\eta} - r(\eta) \end{pmatrix}$$


 FIG. 3. Dependence of beam power  $N$  on the peak amplitude  $\mu$ .

and  $r$  and  $s$  are functions of  $\eta$  defined in terms of  $F$  and  $F'$  as

$$r(\eta) = \frac{-1 + 3\gamma FF' + \gamma F^3 F'}{(1 + F^2)^2},$$

$$s(\eta) = \frac{F^2 - \gamma F^3 F' + \gamma FF'}{(1 + F^2)^2}.$$

The stability of the diffusionless case ( $\gamma=0$  and  $a=0$ ) may be investigated by the well-known *Vakhitov-Kolokolov* criterion [14], which in this case predicts normal mode stability if  $\partial N/\partial B < 0$ . This condition may be rewritten in the form  $N'(\mu)/B'(\mu) < 0$ , where  $N(\mu)$  is easily evaluated as the definite integral,

$$N(\mu) = \int_0^\mu \frac{\mu G^2 dG}{\sqrt{\mu^2 \ln(1 + G^2) - \ln(1 + \mu^2) G^2}}.$$

The derivative  $B'(\mu)$  is negative for all positive  $\mu$  and  $N(\mu)$  is found through the numerical integration to increase monotonically for  $\mu$  in the range  $(0, 40)$ . Results up to  $\mu = 10$  are shown in Fig. 3. Therefore,  $\partial N/\partial B < 0$  and, according to the *Vakhitov-Kolokolov* criterion, all rectilinear screening solitons are stable.

#### IV. THE EVANS FUNCTION METHOD APPLIED TO RECTILINEAR PROPAGATION

The stability problem for  $\gamma=0$  and  $a=0$  may also be treated using the Evans function method. We briefly introduce an approach to the standard Evans function method applied to this case. Stability system (5) for  $\gamma=0$  and  $a=0$  may be written as a system of first-order differential equations given by

$$\frac{dY}{d\eta} = A(\eta, \lambda)Y, \quad (6)$$

where  $Y = (u \ u_\eta \ v \ v_\eta)^T$  and

$$A(\eta, \lambda) = \begin{pmatrix} 0 & 1 & 0 & 0 \\ -B - r(\eta) + \lambda & 0 & -s(\eta) & 0 \\ 0 & 0 & 0 & 1 \\ -s(\eta) & 0 & -B - r(\eta) - \lambda & 0 \end{pmatrix}.$$

As  $\eta \rightarrow \pm\infty$ ,  $r(\eta) \rightarrow -1$ , and  $s(\eta) \rightarrow 0$ , thus the matrix operator tends to a constant matrix  $A_\infty(\lambda)$ . Hence, the asymptotic system has solutions of the form

$$Y_i^\infty(\eta, \lambda) = y_i(\lambda) \exp[\rho_i(\lambda) \eta], \quad i = 1, \dots, 4,$$

where  $\rho_i(\lambda)$  are the eigenvalues of  $A_\infty(\lambda)$  given by  $\pm\sqrt{\omega \pm \lambda}$ , with  $\omega = 1 - B$ , and  $y_i(\lambda)$  are the corresponding eigenvectors. Full problem (6) has four solutions  $Y_i^-$  for which the behavior as  $\eta \rightarrow -\infty$  satisfies  $Y_i^-(\eta, \lambda) \sim Y_i^\infty$  and has also four solutions  $Y_i^+$  for which the behavior as  $\eta \rightarrow +\infty$  satisfies  $Y_i^+(\eta, \lambda) \sim Y_i^\infty$ . Either set of solutions forms a basis for the solution space to Eq. (6). Whenever  $\lambda$  belongs to the set  $S = \{\lambda \in \mathbb{R}; |\lambda| > \omega\}$  two of the values  $\rho_i(\lambda)$  are purely imaginary and the remaining two are real and of opposite sign. For  $\lambda \in S$  there is necessarily an intersection between the subspace spanned by the three solutions bounded at  $+\infty$  and the subspace spanned by the three solutions bounded at  $-\infty$ . This set of eigenfunctions corresponds to the continuous spectrum. There are also isolated eigenvalues occurring in  $\mathbb{C} \setminus S$ , for which the eigenfunctions decay exponentially in both directions. One example is  $\lambda = 0$ , which is always an eigenvalue of algebraic multiplicity equal to 4. This fact is related to the four invariances of evolution equation (1), namely, translations in  $z$  and in  $x$ , Galilean transformation and constant change of phase. For  $\lambda \in \mathbb{C} \setminus S$ , there are always two values of  $\rho_i(\lambda)$  whose real part is positive. Let us denote them by  $\rho_j(\lambda)$  ( $j=1,2$ ). The other two, which we denote by  $\rho_k(\lambda)$  ( $k=3,4$ ), have negative real part. An eigenfunction corresponding to an isolated eigenvalue must be a linear combination of  $Y_1^-(\eta, \lambda)$  and  $Y_2^-(\eta, \lambda)$  and simultaneously a linear combination of  $Y_3^+(\eta, \lambda)$  and  $Y_4^+(\eta, \lambda)$ . In other words, the two pairs of functions should be linearly dependent, that is,

$$a_1 Y_1^-(\eta, \lambda) + a_2 Y_2^-(\eta, \lambda) = a_3 Y_3^+(\eta, \lambda) + a_4 Y_4^+(\eta, \lambda). \quad (7)$$

Here we define the Evans function as the determinant whose columns are  $Y_j^-$  and  $Y_k^+$  evaluated, for instance, at the peak location of  $F$ , which, by the translational invariance of the corresponding ODE [i.e., Eq. (2) with  $a=0$ ,  $\gamma=0$ ], may be chosen as  $\eta=0$ . Thus, the following determinant

$$D(\lambda) = \begin{vmatrix} \vdots & \vdots & \vdots & \vdots \\ Y_1^- & Y_2^- & Y_3^+ & Y_4^+ \\ \vdots & \vdots & \vdots & \vdots \end{vmatrix}_{(0, \lambda)} \quad (8)$$

is an analytic function in  $\lambda$ , which is equal to 0 if and only if Eq. (7) is satisfied, that is, if and only if  $\lambda$  is an eigenvalue of Eq. (5). Moreover, the multiplicity of its 0's coincides with the algebraic multiplicity of the eigenvalues. One important

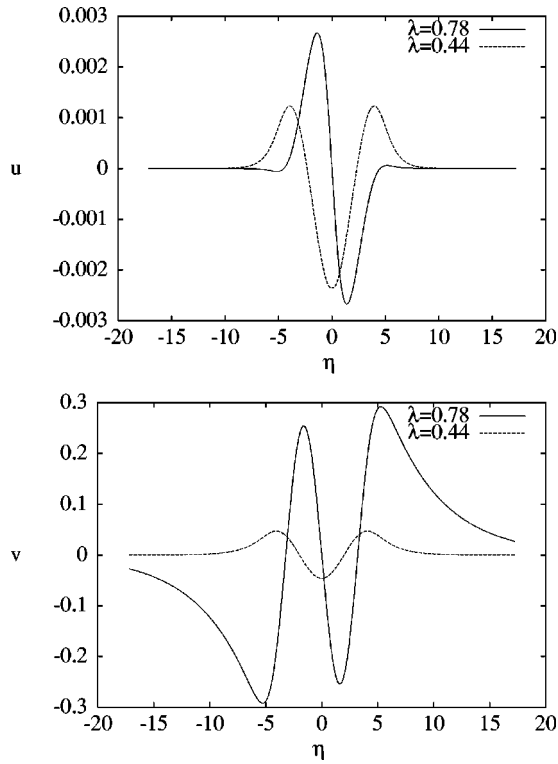


FIG. 4. Perturbations  $u$  and  $v$  that constitute the eigenfunctions corresponding to  $\lambda=0.44$  and  $\lambda=0.78$  for a solution  $F(\eta)$  of amplitude  $\mu=4.0$ .

advantage of this method is based on the analyticity of  $D(\lambda)$ , which permits the use of the argument principle for counting the 0's of  $D(\lambda)$  inside a certain region only by determining the change of  $\arg D(\lambda)$ , as  $D(\lambda)$  is evaluated while  $\lambda$  moves around the boundary of such a region.

The application of the Evans function method to the symmetric beams, up to an amplitude of  $\mu=6.0$ , has confirmed their stability. All the eigenvalues lie on the real axis within the gap of the continuous spectrum. For small amplitudes, up to  $\mu=1.2$ , only the zero eigenvalue exists with the expected algebraic multiplicity equal to 4. Between  $\mu=1.2$  and  $\mu=1.3$ , one pair of symmetrically placed eigenvalues emerges from the continuous spectrum and an increase in amplitude makes these eigenvalues move towards the origin. For higher amplitudes, further pairs of real eigenvalues were observed. For instance, for  $\mu=4.0$  there are two nonzero pairs and for  $\mu=6.0$  there are three nonzero pairs. These nonzero real eigenvalues are characteristic of nonintegrable generalized nonlinear Schrödinger (NLS) models and are usually called *internal modes* [15–17]. The eigenfunctions of the nonzero eigenvalues for  $\mu=4.0$  are shown in Fig. 4. The eigenfunction corresponding to the pair of eigenvalues lower in magnitude is symmetric, while the other is antisymmetric.

### V. THE EVANS FUNCTION METHOD APPLIED TO SELF-BENDING BEAMS

The normal mode stability for the diffusive case is less standard than for the diffusionless case. The numerically obtained profiles for  $F(\psi)$  show rapid decay to 0 in both direc-

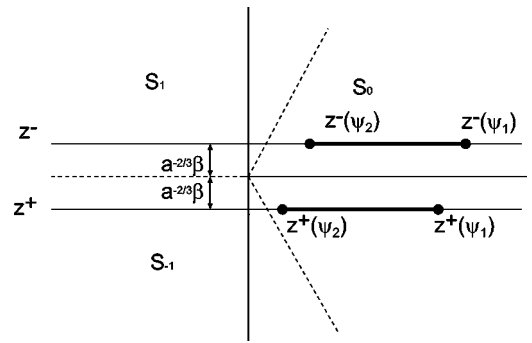


FIG. 5.  $z^\pm$  lines and profile domains  $[z^\pm(\psi_2), z^\pm(\psi_1)]$  for  $\lambda = \alpha - \beta i$ .

tions. Thus, the asymptotic form of eigenvalue problem (5) for the variable  $\psi$  takes the form of two Airy equations for which the independent variables depend on the eigenvalue  $\lambda$ . They read

$$(\partial_{z^+} + z^+ - z^+)u = 0, \quad (\partial_{z^-} - z^- - z^-)v = 0,$$

where  $z^\pm = a^{-2/3}(-a\psi \pm \lambda)$ . The variables  $z^+$  and  $z^-$  are complex, since  $\lambda$  may be complex. For fixed  $\lambda$ , the domain of real  $\psi$  transforms into two parallel lines in the complex plane of  $z^\pm$  (see Fig. 5). The lines lie in opposite half-planes being at equal distance from the real axis. Changing the real part of  $\lambda$  translates  $z^+$  and  $z^-$  along the same line and, consequently, relocates the profile in the  $z^\pm$  domains. Changing the imaginary part of  $\lambda$  translates each line vertically.

For all real  $\lambda$ , the two lines lie within the real axis. The portions corresponding to  $[z^\pm(\psi_2), z^\pm(\psi_1)]$  will be called the profile domains. The profile locations in the  $z^+$  and  $z^-$  domains coincide for  $\lambda=0$  and are on the positive semiaxis, but as the modulus of  $\lambda$  increases they move apart in opposite directions. We define two important sets of real  $\lambda$ .

(1)  $S_1 = \{\lambda \in \mathbb{R} : 0 < |\lambda| < \lambda_1\}$ . For  $\lambda \in S_1$ , both profile domains remain on the positive semiaxis and only solutions having rapid decay in both directions are the candidates as solutions of eigenvalue problem (5). They should match the behavior of  $\text{Ai}(z)$  to the left ( $\psi - \psi^* < 0$ , where  $\psi^*$  is the peak position) and the behavior of  $\text{Bi}(z)$  to the right ( $\psi - \psi^* > 0$ ). Note that, although  $\text{Ai}(z)$  is also a bounded function (with algebraic decay) as  $z \rightarrow -\infty$  ( $\psi \rightarrow +\infty$ ), within and near the profile location it still grows to the left. Hence, we may assert that in  $S_1$  the eigenvalues are discrete.

(2)  $S_2 = \{\lambda \in \mathbb{R} : |\lambda| > \lambda_1 > 0\}$ . For  $\lambda \in S_2$ , one of the profile domains lies on the positive semiaxis and the other one has one or both limits on the negative semiaxis. Here, there exists an extra possible matching Airy function, which is  $\text{Ai}(z)$  to the left of the domain that lies in negative  $z$ . Hence, for any  $\lambda \in S_2$ , there exists a bounded solution to Eq. (5) and we may identify  $S_2$  as the continuous spectrum. We still may divide the set  $S_2$  in two subsets, namely,  $S_{2a} = \{\lambda_1 < |\lambda| < \lambda_2\}$  and  $S_{2b} = \{|\lambda| > \lambda_2\}$ . They correspond to the cases of the profile domain on the left being either only partially or totally on the negative semiaxis, respectively. The division embodies the fact that only for  $\lambda \in S_{2b}$  are the solutions simi-

lar to the solutions in the continuous spectrum of the nondiffusive case and of other similar systems; that is, they are similar to radiation modes.

In order that an eigenvalue may have nonzero imaginary part, the corresponding solution of Eq. (5) should be bounded and should decay exponentially in both directions. This is possible if the solution matches the exponentially decaying Airy functions in each direction. Standard theory [18] involves three Airy functions  $Ai_0(z)$  and  $Ai_{\pm 1}(z)$ , each of which decays exponentially in a  $120^\circ$  sector of the  $z$  plane. In such a sector it is said to be *recessive*. For certain regions of the  $\lambda$  plane, each of the loci  $z^+(\psi)$  and  $z^-(\psi)$  as  $\psi \rightarrow \pm\infty$  remains in a fixed sector as  $\lambda$  varies. One such region is the lower half-plane, which we shall be treating

later. Thus, numerical integration of the eigenvalue problem made within such regions needs to involve only a fixed choice of appropriate recessive Airy functions. In the lower half-plane, they are  $Ai_{-1}(z^+)$  as  $z^+ \rightarrow -\infty$ ,  $Ai_0(z^+)$  as  $z^+ \rightarrow +\infty$ ,  $Ai_1(z^-)$  as  $z^- \rightarrow -\infty$ , and  $Ai_0(z^-)$  as  $z^- \rightarrow +\infty$ .

From the above observations, let us define a modified Evans function. The stability system may also be written as a system of first-order differential equations as

$$\frac{dY}{d\psi} = A(\psi, \lambda)Y, \tag{9}$$

where  $Y = (u \ u_\psi \ v \ v_\psi)^T$  and

$$A(\psi, \lambda) = \begin{pmatrix} 0 & 1 & 0 & 0 \\ -a\psi - 1 - r + \lambda & -\gamma F^2/(1+F^2) & -s & -\gamma F^2/(1+F^2) \\ 0 & 0 & 0 & 1 \\ -s & -\gamma F^2/(1+F^2) & -a\psi - 1 - r - \lambda & -\gamma F^2/(1+F^2) \end{pmatrix}. \tag{10}$$

For  $\lambda \in \{\lambda: \lambda = \alpha + \beta i, \beta < 0\}$ , solutions to the asymptotic system include the following:

$$\begin{aligned} Y_1^\infty(\psi, \lambda) &= (Ai_{-1}(z^+) \quad -a^{1/3}Ai'_{-1}(z^+) \quad 0 \ 0)^T, \\ Y_2^\infty(\psi, \lambda) &= (0 \ 0 \ Ai_1(z^-) \quad -a^{1/3}Ai'_1(z^-))^T, \\ Y_3^\infty(\psi, \lambda) &= (Ai_0(z^+) \quad -a^{1/3}Ai'_0(z^+) \quad 0 \ 0)^T, \\ Y_4^\infty(\psi, \lambda) &= (0 \ 0 \ Ai_0(z^-) \quad -a^{1/3}Ai'_0(z^-))^T. \end{aligned} \tag{11}$$

As for the standard Evans function method described earlier, we construct two bases of solutions to the full problem, one set  $\{Y_k^+\}$  whose behavior at  $+\infty$  satisfies  $Y_k^+(\psi, \lambda) \sim Y_k^\infty$  and the other set  $\{Y_k^-\}$  whose behavior at  $-\infty$  satisfies  $Y_k^-(\psi, \lambda) \sim Y_k^\infty$ . A localized solution exists for  $\lambda$  belonging to the lower half-plane if and only if the determinant

$$D_{ai}(\lambda) = \begin{vmatrix} \vdots & \vdots & \vdots & \vdots \\ Y_1^+ & Y_2^+ & Y_3^- & Y_4^- \\ \vdots & \vdots & \vdots & \vdots \end{vmatrix}_{(\psi^*, \lambda)} \tag{12}$$

is equal to 0. Note that the functions are evaluated at the peak location, here denoted by  $\psi^*$ .  $D_{ai}(\lambda)$  is our modified version of the Evans function and for this to be used as  $D(\lambda)$  we need to prove its analyticity in  $\lambda$ . The Airy functions are entire functions, i.e., functions that are analytic everywhere in  $\mathbb{C}$ , and the variables  $z^\pm$  are analytic functions of  $\lambda$ . The initial conditions for numerical integration from  $\psi_1$  and  $\psi_2$  to  $\psi^*$  are based upon the asymptotic solutions  $Y_k^\infty$ , thus they

are analytic. Consequently, the solutions  $Y_i^+$  ( $i=1,2$ ) and  $Y_j^-$  ( $j=3,4$ ) are also analytic in  $\lambda$ . The determinant is an algebraic operation; therefore,  $D_{ai}(\lambda)$  is analytic in  $\lambda$ .

To prove stability, we need to evaluate  $D_{ai}(\lambda)$  along a closed path enclosing all the lower half-plane of  $\lambda$  [or equivalently the upper half-plane, since the symmetry of Eq. (5) only allows sets of eigenvalues of the kind  $\{\lambda, -\lambda, \lambda^*, -\lambda^*\}$ ]. However, in practice, we have chosen the contour as a semicircle of large radius (typically  $\sim 10$ ) closed by a line parallel to the real axis but very close to it (at distance  $\sim 5 \times 10^{-5}$ ). Numerical limitations are that  $D_{ai}(\lambda)$  appears chaotic for large values of  $|\lambda|$ . The number of 0's of  $D_{ai}(\lambda)$  inside the semicircle was determined by the argument principle. For all profiles studied, the result was that no 0's were found, so confirming the stability of the self-bending solitons.

The defined Evans function was also useful for finding the quasilocalized solutions of Eq. (5), for real  $\lambda$ . One trivial example of those solutions is the profile  $F(\psi)$ , which is the eigenfunction corresponding to the eigenvalue  $\lambda=0$ . The zero eigenvalue is confirmed to have algebraic multiplicity equal to 4 as happens in the diffusionless case. Other solutions for  $\lambda \neq 0$ , if present, are the counterpart of internal modes of the diffusionless case. We have sought for them for  $\lambda$  on the real axis. As  $\lambda$  is real,  $z^\pm$  is also real and we may replace  $Ai_{-1}$  and  $Ai_1$  in Eq. (11) by the real function  $Bi$ . As anticipated, whenever such eigenfunctions exist, they correspond to  $\lambda \in S_1$ . For  $\gamma$  small, such solutions do exist for peak amplitudes greater than  $\sim 1.3$ , as in the diffusionless case. As  $\gamma$  increases and the peak amplitude is maintained, those localized solutions cease to exist. The explanation is that  $S_1$  is narrowing as  $\gamma$  increases. The latter was confirmed by evaluating the value of  $\lambda$  that makes  $z^\pm(\psi_2)=0$  where

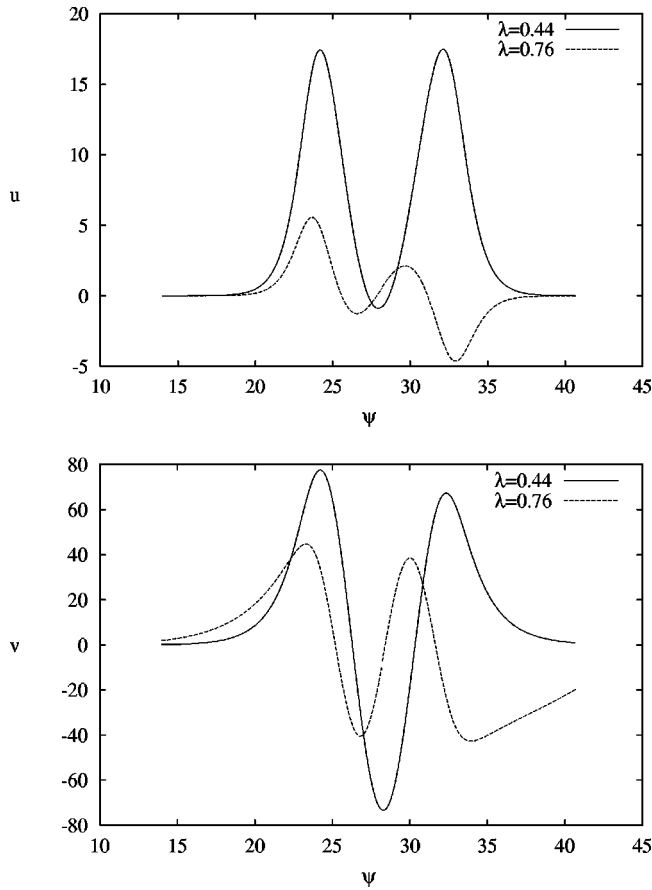


FIG. 6. Eigenfunctions corresponding to  $\lambda=0.76$  and  $\lambda=0.44$  for a beam profile with amplitude  $F_{\max}=4.0$  and  $\gamma=0.03$ .

$\psi_2$  is in the right tail of the peak. Moreover,  $S_1$  tends to the continuous spectrum gap  $(-\omega, \omega)$  of the diffusionless case as  $\gamma$  tends to 0.

Figure 6 shows the localized eigenfunctions found for a beam profile with  $F_{\max}=4.0$  and  $\gamma=0.03$ . They are qualitatively similar to those presented in Fig. 4 for the rectilinear beams, but with noticeable asymmetry. Increasing  $\gamma$  but maintaining  $F_{\max}$  causes the eigenfunction corresponding to  $\lambda=0.76$  to cease to exist. For even larger  $\gamma$ , we were unable to find a solution for the ODE defining  $F$ , suggesting that there is no localized self-similar solution.

## VI. NUMERICAL SIMULATION OF THE PARTIAL DIFFERENTIAL EQUATION

To complement our stability analysis we used the computed beam profiles as initial conditions for numerical integration of evolution equation (1). We used a pseudospectral method based on Fornberg and Whitham [19].

The numerical simulations for  $\gamma=0$  confirmed the stability of the symmetric beams. An initial condition consisting of a self-similar profile plus a small perturbation causes readjustment to a nearby beam shape with some emission of radiation. However, as is typical for other nonintegrable generalized NLS models [15,20], the consequent propagation

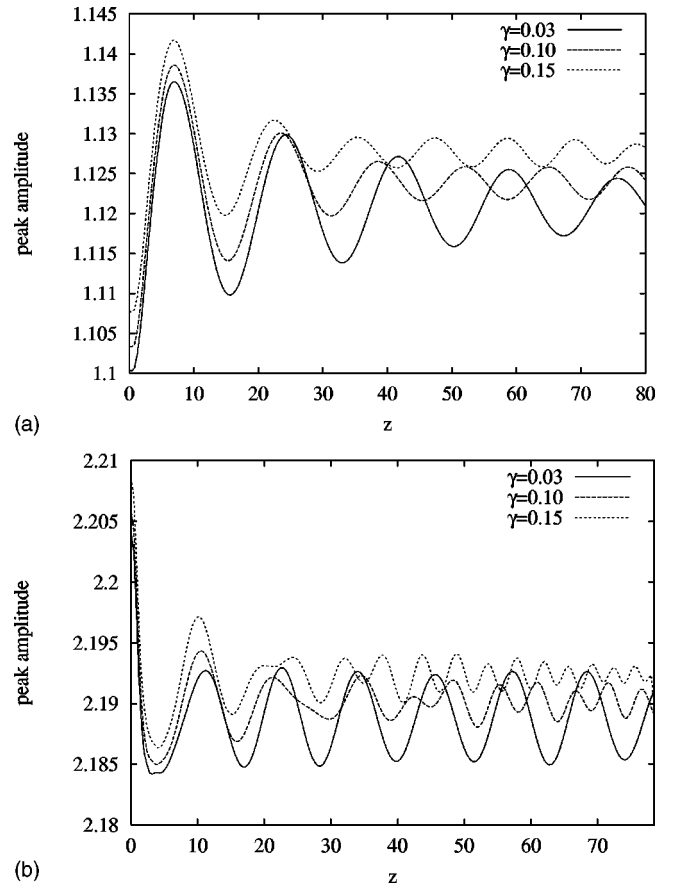


FIG. 7. Peak amplitude evolution for beams scaled by 10% concerning  $\gamma=0.03, 0.10, 0.15$  and (a)  $F_{\max} \sim 1.0$ , (b)  $F_{\max} \sim 2.0$ .

exhibits persistent amplitude oscillations whenever the underlying self-similar beam possesses an internal mode.

The numerical simulations also confirmed the stability of the self-bending beams. We have used the corresponding beam profiles as initial conditions in a way that spans the studied ranges of  $\gamma$  and peak amplitude. In all cases, we have observed steady propagation along the predicted parabolic trajectory. Moreover, stable propagation arises even when initial conditions differ from those of a self-similar profile by small perturbations of three types: a sinusoid multiplying the profile, a multiple of the profile, and a multiple of its first derivative.

Analogously to the diffusionless case, the propagation of perturbed beams reveals the existence or absence of localized modes in their stability spectrum. Thus, we may observe large persistent oscillations in the propagation of beams whose spectrum admits localized modes and smaller decaying oscillations otherwise. The frequency of the decaying oscillations is, in this case, coincident with the limit  $\lambda_2$  of  $S_{2b}$ . As regards the characteristic features of solutions to Eq. (5) for  $\lambda \in S_{2b}$  given above, we may assert also that, when perturbed, the self-bending beams without *internal modes* relax with amplitude oscillations whose frequency is equal to the lowest frequency of their radiationlike modes. Figure 7(a) shows the peak amplitude evolution of solutions of Eq. (4) having  $F_{\max} \sim 1.0$  but scaled by 1.1, for various values of

$\gamma$ . We recall that these profiles have no localized modes except that corresponding to  $\lambda=0$ . The frequency of the amplitude oscillations increases with  $\gamma$  as also does  $\lambda_2$ . In fact,  $\lambda_2$  is estimated in a way similar to  $\lambda_1$ , that is, by evaluation of the value of  $\lambda$  that makes  $z^\pm(\psi_1)=0$ , where  $\psi_1$  is in the left tail of the peak. Furthermore,  $\lambda_2$  also tends to  $\omega$  as  $\gamma$  tends to 0. Figure 7(a) also shows a noticeable decrease in the amplitude of the oscillation with increasing  $\gamma$ . The case  $\gamma=0.03$  of Fig. 7(b) shows the long-lived oscillation whose frequency coincides with the eigenvalue of the localized mode. However, the beams of similar peak amplitude but corresponding to larger diffusion parameter evolve accompanied by decaying oscillations. We have confirmed that the average beams of those latter cases have no localized modes. The frequency of the oscillations is again increasing with  $\gamma$ .

## VII. CONCLUSION

We have proved linear stability for the rectilinear screening solitons and obtained their internal modes. We give a contribution to the stability analysis of the self-bending solitons, including a discussion of their internal modes. This is based on a modified Evans function that deals with asymptotic systems given by Airy equations, instead of constant coefficient differential equations. The modified Evans function procedure may be applied to similar stability problems, as is currently being done.

## ACKNOWLEDGMENTS

M. Fação acknowledges the support of Fundação para a Ciência e a Tecnologia, Portugal.

- 
- [1] M. Segev, B. Crosignani, A. Yariv, and B. Fischer, *Phys. Rev. Lett.* **68**, 923 (1992).
  - [2] G. Duree, J.L. Shultz, G. Salamo, M. Segev, A. Yariv, B. Crosignani, P. DiPorto, E. Sharp, and R.R. Neurgaonkar, *Phys. Rev. Lett.* **71**, 533 (1993).
  - [3] M. Segev, G.C. Valley, B. Crosignani, P. DiPorto, and A. Yariv, *Phys. Rev. Lett.* **73**, 3211 (1994).
  - [4] D.N. Christodoulides and M.I. Carvalho, *J. Opt. Soc. Am. B* **12**, 1628 (1995).
  - [5] M.I. Carvalho, S.R. Singh, and D.N. Christodoulides, *Opt. Commun.* **120**, 311 (1995).
  - [6] W. Krolikowski, N. Akhmediev, B. Luther-Davies, and M. Cronin-Golomb, *Phys. Rev. E* **54**, 5761 (1996).
  - [7] D.F. Parker, C. Sophocleous, and C. Radha, *J. Phys. A* **35**, 1283 (2002).
  - [8] J.W. Evans, *Indiana Univ. Math. J.* **24**, 1169 (1975).
  - [9] J. Alexander, R. Gardner, and C. Jones, *J. Reine Angew. Math.* **410**, 167 (1990).
  - [10] R.L. Pego and M.I. Weinstein, *Philos. Trans. R. Soc. London, Ser. A* **340**, 47 (1992).
  - [11] V.L. Vinetskii and N.V. Kukhtarev, *Sov. Phys. Solid State* **16**, 2414 (1975).
  - [12] N. Kukhtarev, V.B. Markov, S.G. Odulov, M.S. Soskin, and V.L. Vinetskii, *Ferroelectrics* **22**, 949 (1979).
  - [13] V. Aleshkevich, Y. Kartashov, and V. Vysloukh, *Phys. Rev. E* **63**, 016603 (2000).
  - [14] M.G. Vakhitov and A.A. Kolokolov, *Radiophys. Quantum Electron.* **16**, 783 (1973).
  - [15] C. Etrich, U. Peschel, F. Lederer, B.A. Malomed, and Y.S. Kivshar, *Phys. Rev. E* **54**, 4321 (1996).
  - [16] D.E. Pelinovsky, Y.S. Kivshar, and V.V. Afanasjev, *Physica D* **116**, 121 (1998).
  - [17] Y.S. Kivshar, D.E. Pelinovsky, T. Cretegny, and M. Peyrard, *Phys. Rev. Lett.* **80**, 5032 (1998).
  - [18] F.W.J. Olver, *Asymptotics and Special Functions* (A.K. Peters, Wellesley, 1997).
  - [19] B. Fornberg and G.B. Whitham, *Philos. Trans. R. Soc. London, Ser. A* **289**, 373 (1978).
  - [20] V.V. Afanasjev, P.L. Chu, and Y.S. Kivshar, *Opt. Lett.* **22**, 1388 (1997).